Accurate Differential Global Positioning System via Fuzzy Logic Kalman Filter Sensor Fusion Technique

Kazuyuki Kobayashi, Ka C. Cheok, *Member, IEEE*, Kajiro Watanabe, and Fumio Munekata

***Abstract*—The ability to determine an accurate global position of a vehicle has many useful commercial and military applications. The differential global positioning system (DGPS) is one of the practical navigation tools used for this purpose. However, the DGPS has limitations arising from slow updates, signal interference, and limited accuracy. This paper describes how vehicle rate sensors can be used to help a DGPS overcome these limitations. The theoretical background for the sensor fusion is based on the principle of Kalman filtering and a fuzzy logic scheme. Validity of the method was verified by using experimental data from an actual automobile navigating around an urban area. The results demonstrated that the path of the automobile can be continuously traced with high accuracy and repeatability, in spite of the limitations of the DGPS.**

***Index Terms*— Differential global positioning system, fuzzy logic, Kalman filter, sensor fusion.**

I. Introduction

A GLOBAL positioning system (GPS) unit is a compact and easy-to-use positioning system for pinpointing the absolute longitude and latitude coordinates of a position on the earth. It receives radio information from a network of satellites that orbit around the earth. However, low-cost commercial-grade GPS information is subjected to an intentional degradation process called selective availability (SA) [1]. SA is a form of low unpredictable frequency noise artificially introduced by the satellites for security reasons. An error as large as 100 m may be introduced in a GPS measurement by the SA.

Differential GPS (DGPS) [2], on the other hand, is a dual GPS method that uses the concept of a fixed GPS station and a moving GPS station. The method was the fixed GPS station as a point of reference for the moving GPS. By receiving signals from the same satellites, it is able to eliminate the effect of SA and calculate the relative coordinates between the two stations. Thus, a commercial GPS yields rough absolute coordinates of a position, while the DGPS yields accurate relative coordinates between two GPS positions.

Both the GPS and the DGPS share the problem of slow updates. Moreover, they sometimes cannot receive information from the satellites for minutes at a time, due to radio interference or loss of signals. Absence of GPS radio waves means that the position of the unit cannot be identified.

To overcome these limitations, several sensor fusion methods have been proposed for enhancing the reliability of the GPS. For example, a map-matching technique using an optical rate gyro and wheel speed sensor [3] was combined with the GPS to reduce the effects of radio interference and noise [4]. A drawback in using map matching is that it sometimes fails to locate the vehicle position in areas with congested roads and crowded buildings or objects. Reference [5] describes a more elaborate multisensor approach using an inertial navigation system (INS), altimeter, and other positioning system, LORAN-C, GLONASS, to improve the accuracy of GPS and also to provide a fault diagnosis function. However, this system is expensive and impractical for automobile applications.

In this paper, we present a fuzzy-logic-tuned Kalman filter (FLKF) sensor fusion technique that appropriately combines measurements from a vehicle DGPS with a yaw-rate gyro and a speed sensor according to the reliability of the sensor information. The Kalman filter equation builds on a dynamical relationship among the sensors, while the fuzzy logic tunes the parameters of the Kalman filter algorithm. We also employ a complex variable technique for the Kalman filtering algorithm to reduce the computational load.

Experiments were carried out to acquire data from the DGPS and rate sensors on board automobiles. We use the experimental data to evaluate how the proposed technique can simultaneously handle the high-frequency noise from the sensors and the frequent information interference in the DGPS. The experimental results demonstrate the effectiveness of the FLKF. As shown in this paper, the FLKF traces out the path taken by the automobile with consistent accuracy and repeatability.

Section II of this paper describes the sensor fusion arrangements for the global positioning problem. We provide a mathematical and analytical basis in Section III. The promising experimental results are reported in Section IV, and a conclusion is provided in Section V.

II. Problem Description

A. Differential GPS and Vehicle Rate Sensors

Fig. 1 shows the proposed positioning system. Both the fixed-base GPS station and the GPS on board the moving

Manuscript received March 22, 1996; revised November 18, 1997.

K. Kobayashi was with the Department of Electrical and System Engineering, School of Engineering and Computer Science, Oakland University, Rochester, MI 48309-4401 USA. He is now with the Department of System and Control Engineering, College of Engineering, Hosei University, Tokyo, 184 Japan.

K. C. Cheok is with the Department of Electrical and System Engineering, School of Engineering and Computer Science, Oakland University, Rochester, MI 48309-4401 USA.

K. Watanabe is with the Department of System and Control Engineering, College of Engineering, Hosei University, Tokyo, 184 Japan.

F. Munekata was with the Instrument and Control Engineering Department, College of Engineering, Hosei University, Tokyo, 184 Japan. He is now with NAMCO Ltd., No. 1 Product Development Division, Engineering Department, Yokohama R&D Center, Kanagawa, 224 Japan.

Publisher Item Identifier S 0278-0046(98)03544-8.

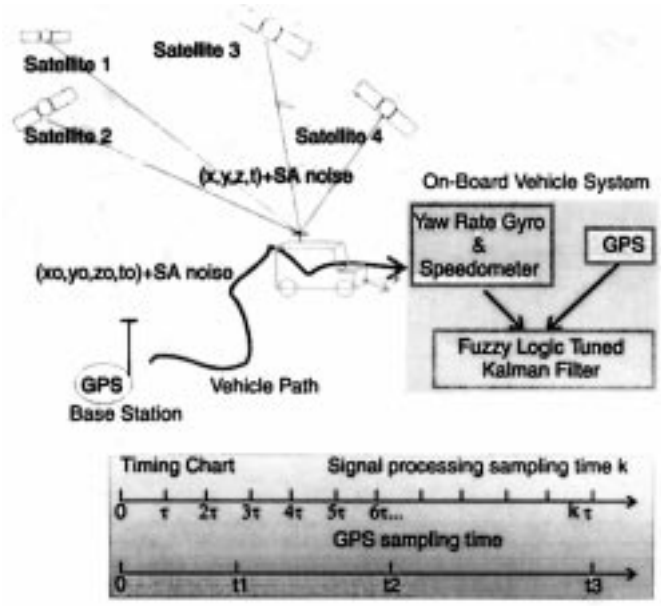

Fig. 1. Configuration for proposed global positioning scheme.

vehicle receive signals from the same satellites. The satellite information of each contains the SA degradation. The DGPS process removes the SA noise and provides the relative position of the vehicles, obtained by subtracting the coordinates of the fixed station from that of the moving vehicle. The FLKF is used to discriminate and extract useful information from the yaw-rate gyro, speedometer, and DGPS. The goal is to have the output of the FLKF trace out the path taken by the vehicle.

The timing diagram for receiving information from the DGPS and vehicle sensors is also shown in Fig. 1. The updates from the sensors are much faster and regular, while the updates from the DGPS are less frequent and may be asynchronous. The variables and constants for the proposed positioning system in Fig. 1 and subsequent formulations are as follows:

Common Variables and Constants:

- t_k time instance when GPS information is updated (asynchronous);
- τ sampling interval for the Kalman filter;
- t continuous time;
- k discrete-time index for the Kalman filter.

Earth Coordinate System:

- $[x(k)\ y(k)]$ position coordinates of the vehicle;
- $v(t)$ forward speed of the vehicle;
- $v_m(t)$ measurement forward speed of the vehicle from speedometer;
- $[v_x(k)\ v_y(k)]$ x–y component of vehicle speed;
- $\omega(t)$ yaw rate of the vehicle;
- $\theta(k)$ angular direction of the vehicle at time $t = k\tau$;
- θ_0 initial direction of the vehicle;
- $\Delta\theta(k+1)$ angle moved in the time interval from to $+1$;
- $\Delta\theta_m(k+1)$ measurement angle from yaw-rate gyro;
- $\xi(k) = \cos\theta(k)$ x component of direction unit vector;
- $\zeta(k) = \sin\theta(k)$ y component of direction unit vector.

Noise Variables and Parameters:

- $w_v(k)$ measurement errors associated with $v_m(k)$;
- $v_{\Delta\theta}(k)$ measurement errors associated with $\Delta\theta_m(k)$;
- $Q_v(k)$ covariance of $w_v(k)$;
- $Q_{\Delta\theta}(k)$ covariance of $w_{\Delta\theta}(k)$;
- $w_1(k)\cdots w_6(k)$ system noise due to $w_v(k)$ and $w_{\Delta\theta}(k)$;
- $[x_m(k)\ y_m(k)]$ coordinate measurement signals from vehicle DGPS;
- $[n_x(k)\ n_y(k)$ measurement noise for $[x_m(k)\ y_m(k)]$;
- $R_x(k), R_y(k)$ covariance of $n_x(k), n_y(k)$.

Complex Kalman Filter:

- $\boldsymbol{z}(k)$ complex variable representation for measurement signals $[x_m(k)\ y_m(k)]$;
- $\boldsymbol{n}(k)$ complex variable representation for measurement noise $[n_x(k)\ n_y(k)]$;
- $\boldsymbol{x}(k)$ complex state variable vector;
- $\boldsymbol{w}(k)$ system noise vector;
- $\boldsymbol{A}(k)$ complex time-varying system matrix;
- $\boldsymbol{B}(k)$ complex system noise matrix;
- $\boldsymbol{C}$ output matrix;
- $\boldsymbol{P}(k)$ complex covariance matrix estimation error by Kalman filter;
- $\boldsymbol{M}(k)$ complex coefficient matrix;
- $\boldsymbol{R}(k)$ complex expression of variance $R_x(k), R_y(k)$;
- $\boldsymbol{Q}(k)$ complex covariance matrix of system noise.

B. Assumptions and Problem Description

For the DGPS and vehicle sensors shown in Fig. 1, we assume

A1) Both the fixed and moving GPS receive signals from the same (at least) three or more satellites.

A2) Sampling rate of the gyro and speedometer is sufficiently fast in comparison with the changing rates of the vehicle's angular and forward velocities.

A3) Measurement noise from the vehicle sensors are zero-mean Gaussian white noise.

A4) The gradients in the road profiles are insignificant.

Assumption A1) is a required condition for the DGPS operation. We note that a single fixed-base GPS station will be sufficient for application over a small area, while a few fixed stations may be required to cover a larger area. Assumption A2) can be easily satisfied with a normal microcontroller. Assumption A3) is experimentally supported by the fact that the DGPS, gyro, and speedometer actually have negligible offsets and low-frequency drifts. Assumption A4) is valid for normal city and country roads.

The objective is to design a positioning system that extrapolates the path of the vehicle, even when the satellite signals cannot be received for minutes at a time. We will accomplish this by fusing the yaw-rate gyro and speedometer measurements with the signals from the DGPS using the FLKF

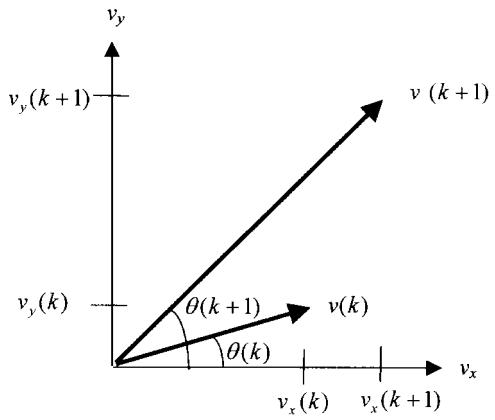

Fig. 2. Relative coordinate system for vehicle.

technique. The task for this problem may be grouped as follows.

P1) Build a mathematical dynamics model to relate the measurements from the rate sensors and the DGPS.

P2) Characterize the measurement noise and the system noise.

P3) Design a Kalman filter algorithm.

P4) Specify fuzzy logic rules for tuning the coefficients of the Kalman filter.

P5) Verify the validity of the method by experiments using an actual automobile.

III. Positioning System by Sensor Fusion

A. Mathematical Formulation

Fig. 2 shows the coordinate system for the position and velocity of the vehicle. The angular direction of the vehicle is calculated from

$$\Delta\theta(k+1) = \int_{k\tau}^{(k+1)\tau} \omega(t)\,dt \tag{1}$$

$$\theta(k+1) = \theta(k) + \Delta\theta(k+1). \tag{2}$$

The x–y velocity is calculated as

$$v_x(k+1) = v(k+1)\cdot\cos\theta(k+1) \tag{3}$$

$$v_y(k+1) = v(k+1)\cdot\sin\theta(k+1). \tag{4}$$

From assumption A2), the coordinate $[x(k+1)\ y(k+1)]$ is calculated or approximated by

$$\begin{aligned} x(k+1) &= x(k) + \tau\cdot v_x(k) \\ y(k+1) &= y(k) + \tau\cdot v_y(k). \end{aligned} \tag{5}$$

Equation (2) yields

$$\begin{aligned} \cos\theta(k+1) &= \cos\{\theta(k) + \Delta\theta(k+1)\} \\ &= \cos\theta(k)\cos\Delta\theta(k+1) \\ &\quad - \sin\theta(k)\sin\Delta\theta(k+1) \\ \sin\theta(k+1) &= \sin\{\theta(k) + \Delta\theta(k+1)\} \\ &= \cos\theta(k)\sin\Delta\theta(k+1) \\ &\quad + \sin\theta(k)\cos\Delta\theta(k+1). \end{aligned} \tag{6}$$

Since we defined $\eta(k) = \sin\theta(k)$ and $\xi(k) = \cos\theta(k)$, a time-varying discrete state-variable equation for the above can be derived as (7), shown at the bottom of the page.

B. System and Measurement Noise

If we use the measurements from the rate sensors as parameters in (7), we would obtain (8a), shown at the bottom of the page, where the system noises $w_1(k)\cdot w_6(k)$ can be approximated to a first order by

$$\begin{bmatrix} w_1(k) \\ w_2(k) \\ w_3(k) \\ w_4(k) \\ w_5(k) \\ w_6(k) \end{bmatrix} = \begin{bmatrix} 0 & 0 \\ 0 & 0 \\ \xi(k+1) & -v_m(k+1)\eta(k+1) \\ \eta(k+1) & v_m(k+1)\xi(k+1) \\ 0 & \eta(k+1) \\ 0 & \xi(k+1) \end{bmatrix} \begin{bmatrix} w_v(k) \\ w_{\Delta\theta}(k) \end{bmatrix}. \tag{8b}$$

$$\begin{bmatrix} x(k+1) \\ y(k+1) \\ v_x(k+1) \\ v_y(k+1) \\ \xi(k+1) \\ \eta(k+1) \end{bmatrix} = \begin{bmatrix} 1 & 0 & \tau & 0 & 0 & 0 \\ 0 & 1 & 0 & \tau & 0 & 0 \\ 0 & 0 & 0 & 0 & v(k+1)\cos\Delta\theta(k+1) & -v(k+1)\sin\Delta\theta(k+1) \\ 0 & 0 & 0 & 0 & v(k+1)\sin\Delta\theta(k-1) & v(k+1)\cos\Delta\theta(k+1) \\ 0 & 0 & 0 & 0 & \cos\Delta\theta(k+1) & -\sin\Delta\theta(k+1) \\ 0 & 0 & 0 & 0 & \sin\Delta\theta(k+1) & \cos\Delta\theta(k+1) \end{bmatrix} \begin{bmatrix} x(k) \\ y(k) \\ v_x(k) \\ v_y(k) \\ \xi(k) \\ \eta(k) \end{bmatrix} \tag{7}$$

$$\begin{bmatrix} x(k+1) \\ y(k+1) \\ v_x(k+1) \\ v_y(k+1) \\ \xi(k+1) \\ \eta(k+1) \end{bmatrix} = \begin{bmatrix} 1 & 0 & \tau & 0 & 0 & 0 \\ 0 & 1 & 0 & \tau & 0 & 0 \\ 0 & 0 & 0 & 0 & v_m(k+1)\cos\Delta\theta_m(k+1) & -v_m(k+1)\sin\Delta\theta_m(k+1) \\ 0 & 0 & 0 & 0 & v_m(k+1)\sin\Delta\theta_m(k-1) & v_m(k+1)\cos\Delta\theta_m(k+1) \\ 0 & 0 & 0 & 0 & \cos\Delta\theta_m(k+1) & -\sin\Delta\theta_m(k+1) \\ 0 & 0 & 0 & 0 & \sin\Delta\theta_m(k+1) & \cos\Delta\theta_m(k+1) \end{bmatrix} \begin{bmatrix} x(k) \\ y(k) \\ v_x(k) \\ v_y(k) \\ \xi(k) \\ \eta(k) \end{bmatrix} + \begin{bmatrix} w_1(k) \\ w_2(k) \\ w_3(k) \\ w_4(k) \\ w_5(k) \\ w_6(k) \end{bmatrix} \tag{8a}$$

The noise $w_{\Delta\theta}(k)$ and $w_v(k)$ are measurement noise of the yaw-rate gyro and the speedometer. Their covariance, defined as

$$\sigma^2\{w_{\Delta\theta}(k)\} = Q_{\Delta\beta}, \quad \sigma^2\{w_v(k)\} = Q_v \tag{9}$$

will be tuned according to the estimation conditions given by

$$\xi^2(k) + \eta^2(k) = 1 \tag{10}$$

$$v_x^2(k) + v_y^2(k) = v_m^2(k). \tag{11}$$

The fuzzy logic rule for the tuning is given in the next section.

As shown in Fig. 1, a direct method for determining the position of the vehicle is the information from the DGPS. New DGPS information is available every few seconds. However, a signal from the satellite may become unavailable for an unpredictable length of time due to radio interference or transmission loss. The DGPS measurements can be described by

$$\begin{bmatrix} x_m(k) \\ y_m(k) \end{bmatrix} = \begin{bmatrix} 1 & 0 & 0 & 0 & 0 & 0 \\ 0 & 1 & 0 & 0 & 0 & 0 \end{bmatrix} \begin{bmatrix} x(k) \\ y(k) \\ v_x(k) \\ v_y(k) \\ \xi(k) \\ \eta(k) \end{bmatrix} + \begin{bmatrix} n_x(k) \\ n_y(k) \end{bmatrix}. \tag{12}$$

The measurement noises, $n_x(k)$ and $n_y(k)$, will be used to model the possible errors associated with the satellite information. The first error contained in the DGPS readings x_m and y_m is the error due to geometric positions of the satellites at the time. An indication of the extent of this error is given by a geometrical dilution of precision (GDOP) index, which is additional information transmitted to the GPS by the satellites at every update. The second error in x_m and y_m comes from the error due to lack of updates and asynchronous timing. The magnitude of this type of error increases with the distance ($Distance = \int_{t_k}^{k\tau - t_k} v(t)\, dt$) the vehicle moves in the time interval between DGPS updates. The GDOP index and the *Distance* calculation will be used to determine the variance $R_x(k)$ and $R_y(k)$ for the noise $n_x(k)$ and $n_y(k)$. This is explained by the *Fuzzy Logic Rule Set 1* and (16) described in the next section.

C. Complex Kalman Filter

A Kalman filter can be applied to (8) and (12) to estimate the coordinates of the vehicle position. To reduce calculation time and express the equations in a compact form, we consider the formulation of the Kalman filter in complex variable domain. A complex Kalman filter can reduce calculation time to 70% of time taken by a conventional Kalman filter. We define the complex vectors and matrices as follows, where i denotes the imaginary unit component:

$$\begin{aligned}
\boldsymbol{x}(k) &= [x(k) + i \cdot y(k) \quad v_x(k) + i \cdot v_y(k) \\
&\qquad \xi(k) + i \cdot \eta(k)]^T \\
\boldsymbol{z}(k) &= x_m(k) + i \cdot y_m(k) \\
\boldsymbol{w}(k) &= [w_v(k) \quad w_{\Delta\theta}(k)]^T \\
\boldsymbol{n}(k) &= n_x(k) + i \cdot n_y(k) \\
\boldsymbol{A}(k+1) &= \begin{bmatrix} 1 & \tau & 0 \\ 0 & 0 & v(k+1) \cdot e^{i\Delta\theta(k+1)} \\ 0 & 0 & e^{i\Delta\theta(k+1)} \end{bmatrix} \\
\boldsymbol{B}(k+1) &= \begin{bmatrix} 0 & 0 \\ e^{i\theta(k+1)} & i \cdot v(k+1) \cdot e^{i\theta(k+1)} \\ 0 & i \cdot e^{i\theta(k+1)} \end{bmatrix} \\
\boldsymbol{C} &= [1 \quad 0 \quad 0] \\
\boldsymbol{R}(k) &= R_x(k) = R_y(k) \\
\boldsymbol{Q}(k) &= \begin{bmatrix} Q_v(k) & 0 \\ 0 & Q_{\Delta\theta}(k) \end{bmatrix}.
\end{aligned} \tag{13}$$

Then, (6)–(8) can be more compactly rewritten as a time-varying discrete complex state-variable equation:

$$\begin{aligned}
\boldsymbol{x}(k+1) &= \boldsymbol{A}(k+1)\boldsymbol{x}(k) + \boldsymbol{B}(k+1)\boldsymbol{w}(k) \\
\boldsymbol{z}(k) &= \boldsymbol{C}\boldsymbol{x}(k) + \boldsymbol{n}(k).
\end{aligned} \tag{14}$$

The complex Kalman filter [7] for (14) is described by

$$\begin{aligned}
\hat{\boldsymbol{x}}(k+1) &= \boldsymbol{A}(k+1)\hat{\boldsymbol{x}}(k) + \boldsymbol{P}(k+1)\boldsymbol{C}^{\boldsymbol{T}}\boldsymbol{R}(k+1)^{-1} \\
&\qquad \cdot [\boldsymbol{z}(k+1) - \boldsymbol{C}\boldsymbol{A}(k+1)\hat{\boldsymbol{x}}(k)] \\
\hat{\boldsymbol{x}}(0) &= \boldsymbol{x}_0 \\
\boldsymbol{P}(k) &= \boldsymbol{M}(k) - \boldsymbol{M}(k)\boldsymbol{C}^{\boldsymbol{T}}[\boldsymbol{C}\boldsymbol{M}(k)\boldsymbol{C}^T + \boldsymbol{R}(k)]^T\boldsymbol{C}\boldsymbol{M}(k) \\
\boldsymbol{P}(0) &= \boldsymbol{P}_0 \\
\boldsymbol{M}(k) &= \boldsymbol{A}(k)\boldsymbol{P}(k-1)\boldsymbol{A}^*(k) + \boldsymbol{B}(k)\boldsymbol{Q}(k-1)\boldsymbol{B}^*(k)
\end{aligned} \tag{15}$$

where * denotes the complex conjugate transpose operation.

D. Fuzzy Logic Tuning Rule

The covariance factors for the Kalman filter will be adjusted according to the following simple rules based on the constraint to the system equation and limitation of the sensors. By choosing $\boldsymbol{P}(k), \boldsymbol{Q}(k)$, and $\boldsymbol{R}(k)$ appropriately, the effects of error due to the consistent and sensor inaccuracies are minimized by the Kalman filtering process. The basic tuning idea is as follows.

A check for accuracy of the Kalman filter result can be done by evaluating to see if the estimates $\hat{\xi}(k)$ and $\hat{\eta}(k)$ satisfy the trigonometric identity given by (11) in Section III-B. Deviation of the term $\hat{xi}^2(k) + \hat{\eta}^2(k)$ from unity would indicate poor estimation by the filter. In this case, we may want to increase the covariance coefficient $Q_{\Delta\theta}(k)$. Similarly, accurate estimates $\hat{v}_x(k)$ and $\hat{v}_x(k)$ should approximately satisfy (11).

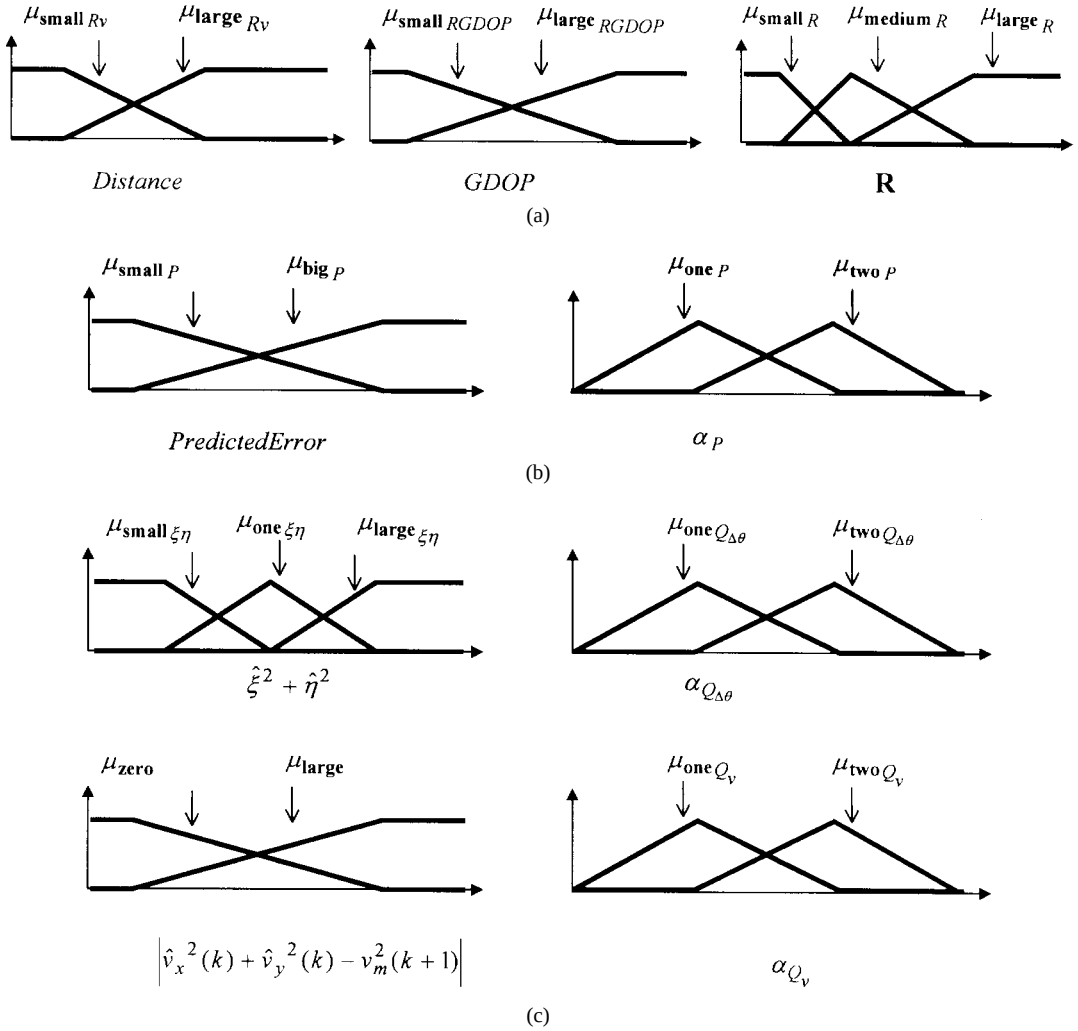

Fig. 3. (a) General membership functions for *Fuzzy Rule Set 1*. (b) General membership functions for *Fuzzy Rule Set 2*. (c) General membership functions for *Fuzzy Rule Set 3*.

Deviation of $\hat{v}_x^2(k) + \hat{v}_y^2(k)$ from $v_m^2(k)$ would indicate poor estimation by the filter and we may increase $Q_v(k)$.

As described in Section III-B, the filter may also adapt to the satellite condition by changing the covariance $R(k)$ as a function of the arguments *GDOP* and *Distance*. In addition, another adaptation for accommodating unavailable GPS signals is to reset the covariance matrix $P(k)$ of the state estimation error when there is an absence of useful satellite data. Based on the above argument, a general fuzzy logic guideline for tuning the Kalman filter is as follows.

Rule Set 1—Tuning of R to handle the DGPS and rate measurement condition

$$If\ Distance(k)\ is\ \mathbf{small}_{Rv}\ and\ GDOP(k)\ is\ \mathbf{small}_{RGDOP}\ then\ \boldsymbol{R}(k)\ is\ \mathbf{small}_R.$$
$$If\ Distance(k)\ is\ \mathbf{small}_{Rv}\ and\ GDOP(k)\ is\ \mathbf{large}_{RGDOP}\ then\ \boldsymbol{R}(k)\ is\ \mathbf{medium}_R.$$
$$If\ Distance(k)\ is\ \mathbf{large}_{Rv}\ and\ GDOP(k)\ is\ \mathbf{small}_{RGDOP}\ then\ \boldsymbol{R}(k)\ is\ \mathbf{large}_R.$$
$$If\ Distance(k)\ is\ \mathbf{large}_{Rv}\ and\ GDOP(k)\ is\ \mathbf{large}_{RGDOP}\ then\ \boldsymbol{R}(k)\ is\ \mathbf{large}_R$$

where $Distance(k) = \int_{k-1}^{t_k} v_m(t)\,dt$ is the distance traveled

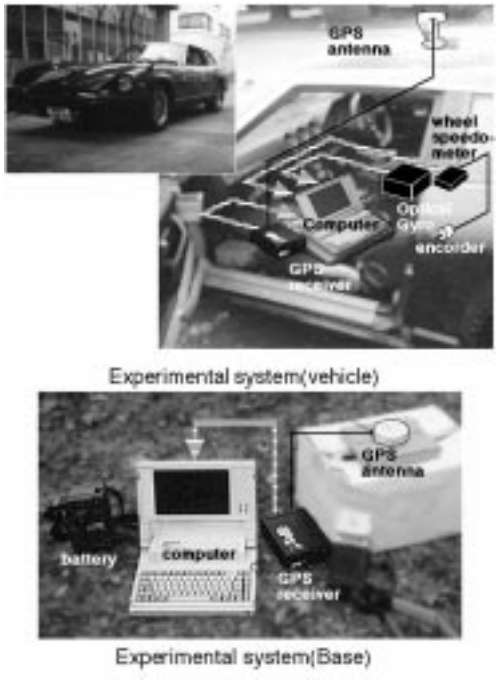

Fig. 4. Experimental system.

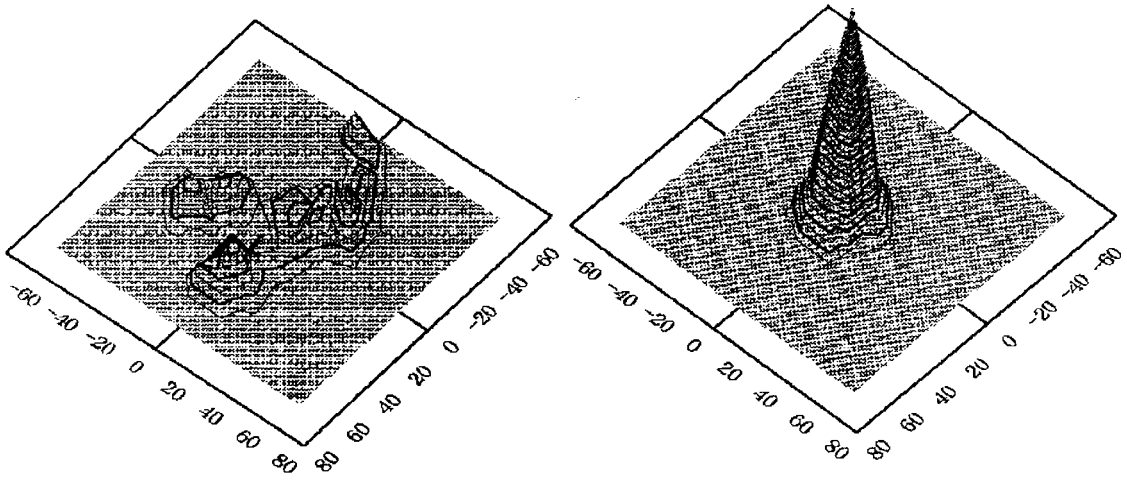

(a) (b)

Fig. 5. Two-dimensional histogram of GPS and DGPS noises.

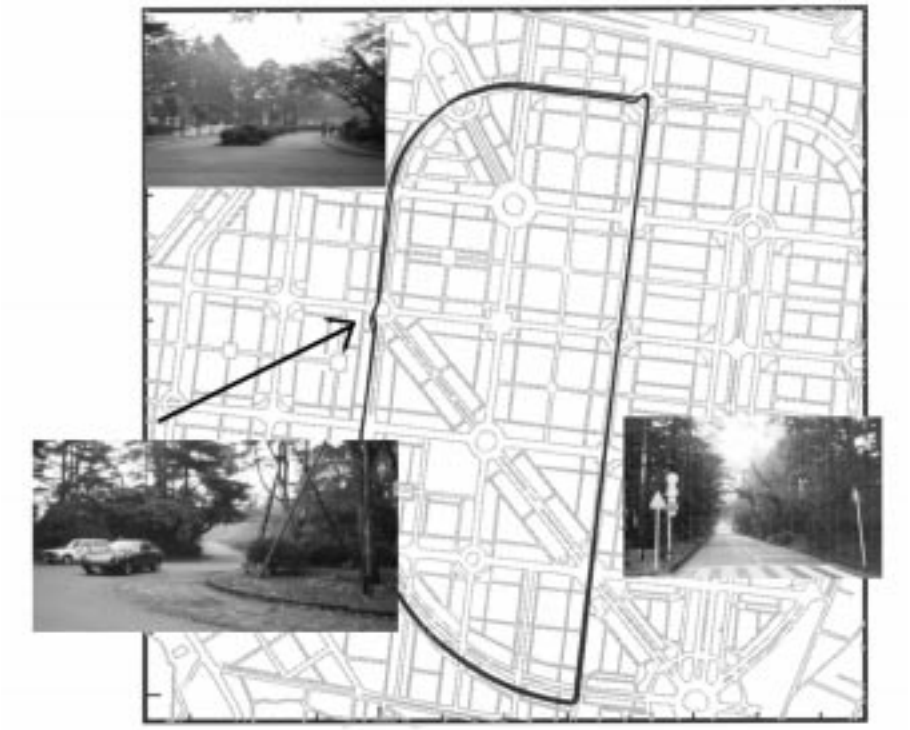

Fig. 6. The course used for experimentation.

by the vehicle in the interval between time instances t_{k-1} and t_k, and $GDOP(k)$ is the received $GDOP$ value at t_k.

Rule Set 2—Tuning of P to handle slow update by DGPS

$If\ PredidcterError(k)\ is\ \mathbf{big}_P\ then\ multiply$
$\boldsymbol{P}(k)\ by\ \mathbf{two}_P.$
$If\ PredidcterError(k)\ is\ \mathbf{small}_P\ then\ multiply$
$\boldsymbol{P}(k)\ by\ \mathbf{one}_P$

where $PredicterError(k) = |\boldsymbol{z}(k) - \boldsymbol{C}\boldsymbol{A}(k+1)\hat{\boldsymbol{x}}(k)|$ is the predicted estimation error at time instance t_k.

Rule Set 3: Tuning of Q to handle consistency in estimation

$If\ \hat{\xi}^2(k) + \hat{\eta}^2(k)\ is\ \mathbf{one}_{\xi\eta}\ then\ multiply$
$Q_{\Delta\theta}(k)\ by\ \mathbf{one}_{Q\Delta\theta}.$
$If\ \hat{\xi}^2(k) + \hat{\eta}^2(k)\ is\ \mathbf{small}_{\xi\eta}\ then\ multiply$
$Q_{\Delta\theta}(k)\ by\ \mathbf{two}_{Q\Delta\theta}.$
$If\ \hat{\xi}^2(k) + \hat{\eta}^2(k)\ is\ \mathbf{large}_{\xi\eta}\ then\ multiply$
$Q_{\Delta\theta}(k)\ by\ \mathbf{two}_{Q\Delta\theta}$

and

$$If\ |\hat{v}_x^2(k)+\hat{v}_y^2(k)-v_m^2(k+1)|\ is\ \mathbf{zero}_v\ then\ multiply\ Q_v(k)\ by\ \mathbf{one}_{Qv}.$$
$$If\ |\hat{v}_x^2(k)+\hat{v}_y^2(k)-v_m^2(k+1)|\ is\ \mathbf{large}_v\ then\ multiply\ Q_v(k)\ by\ \mathbf{two}_{Qv}.$$

Fig. 3 shows the general shapes of membership functions which define the degree or extent to which the fuzzy variables belong to the fuzzy sets. Using a Mamdani-style inference mechanism [8]–[10] with product and center of gravity operation, the output of *Fuzzy Rule Set 1* at the time instance t_k can be expressed as

$$\begin{aligned}
C_1(R,k) &= \mu_{\mathbf{small}\ Rv}(Distance(k)) \\
&\quad \mu_{\mathbf{small}\ RDGOP}(GDOP(k)) \times \mu_{\mathbf{small}\ R}(R) \\
C_2(R,k) &= \mu_{\mathbf{small}\ Rv}(Distance(k)) \\
&\quad \mu_{\mathbf{large}\ RDGOP}(GDOP(k)) \times \mu_{\mathbf{medium}\ R}(R) \\
C_3(R,k) &= \mu_{\mathbf{large}\ Rv}(Distance(k)) \\
&\quad \mu_{\mathbf{Small}\ RDGOP}(GDOP(k)) \times \mu_{\mathbf{large}\ R}(R) \\
C_4(R,k) &= \mu_{\mathbf{large}\ Rv}(Distance(k)) \\
&\quad \mu_{\mathbf{large}\ RDGOP}(GDOP(k)) \times \mu_{\mathbf{large}\ R}(R) \\
R(k) &= \frac{\sum_{j=1}^{4} \int (C_j(R,k)R)\, dR}{\sum_{j=1}^{4} \int C_j(R,k)\, dR}. \qquad (16)
\end{aligned}$$

Next, using a mixed Mamdami–Sugeno-style inference mechanism, the *Fuzzy Rule Set 2* for modifying the calculated Kalman filter error covariance matrix $P(k)$ at t_k can be expressed as

$$\begin{aligned}
C_5(\alpha_P,k) &= \mu_{\mathbf{big}\ P}(PredictedError(k)) \times \mu_{\mathbf{two}\ P}(\alpha_P) \\
C_6(\alpha_P,k) &= \mu_{\mathbf{small}\ P}(PredictedError(k)) \times \mu_{\mathbf{two}\ P}(\alpha_P) \\
P(k) &= \frac{\sum_{j=5}^{6} \int (C_j(\alpha_P,k)\alpha_P)\, d\alpha_P)}{\sum_{j=5}^{6} \int C_j(\alpha_P,k)\, d\alpha_P}. \qquad (17)
\end{aligned}$$

The inference mechanism for *Fuzzy Rule Set 3* can be expressed in a similar manner. Further details on the inference mechanism of fuzzy logic (fuzzification, rule interpretation, and defuzzification) can be found in [8]–[10].

The membership functions for the fuzzy variables ($\mathbf{small}_{Rv}, \mathbf{large}_{Rv}$, etc.) were selected through careful interpretation of the sensor information and fine tuned using *experimental data-driven simulation* as follows. Test experiments were conducted with the vehicle driven over a known test course to record data from the DGPS, yaw-rate gyro, and speedometer on board the vehicle. Simulations of the Kalman filter and the proposed fusion technique were then conducted using the collected data to tune the desired membership functions. The final fuzzy logic will reflect the way a designer would tune the covariance of the Kalman filter to adapt to the reliability of the received information.

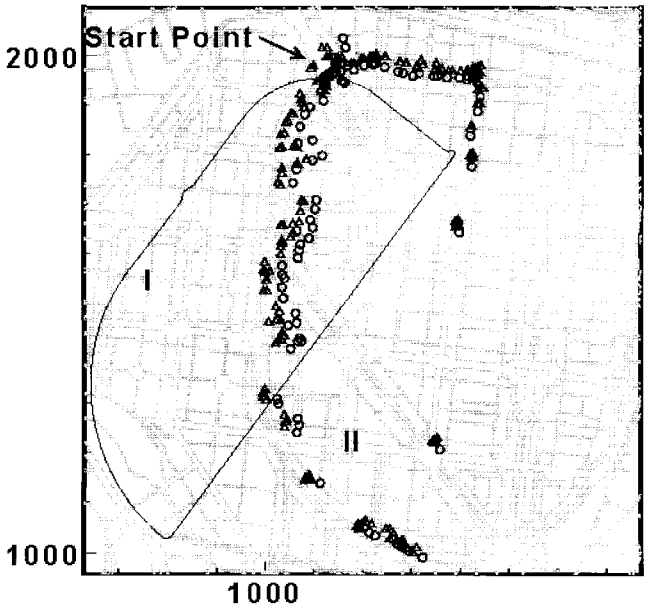

Fig. 7. Trajectories measured by vehicle rate sensors (solid line), GPS (Δ) and DGPS (O). Note that the unit of the axes is in meters. (a) GPS Trajectory. (b) DGPS Trajectory.

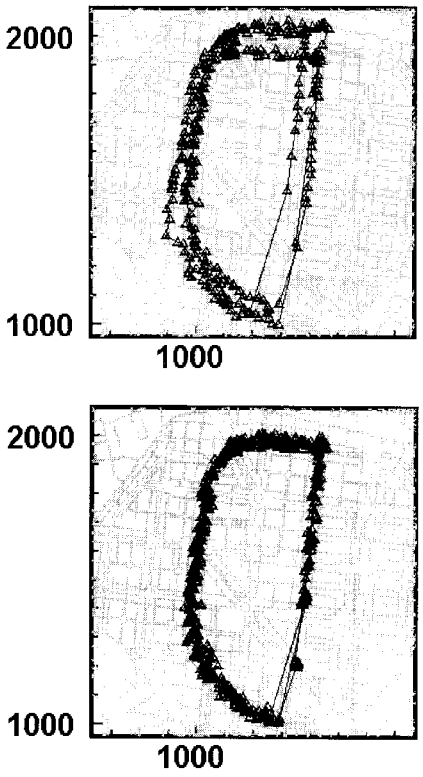

Fig. 8. Experimental demonstration of the degradation effect of SA in GPS and DGPS.

IV. Experiments

A. Experimental System

Fig. 4 shows the experimental system. The basic specifications for the experimental system are as follows.

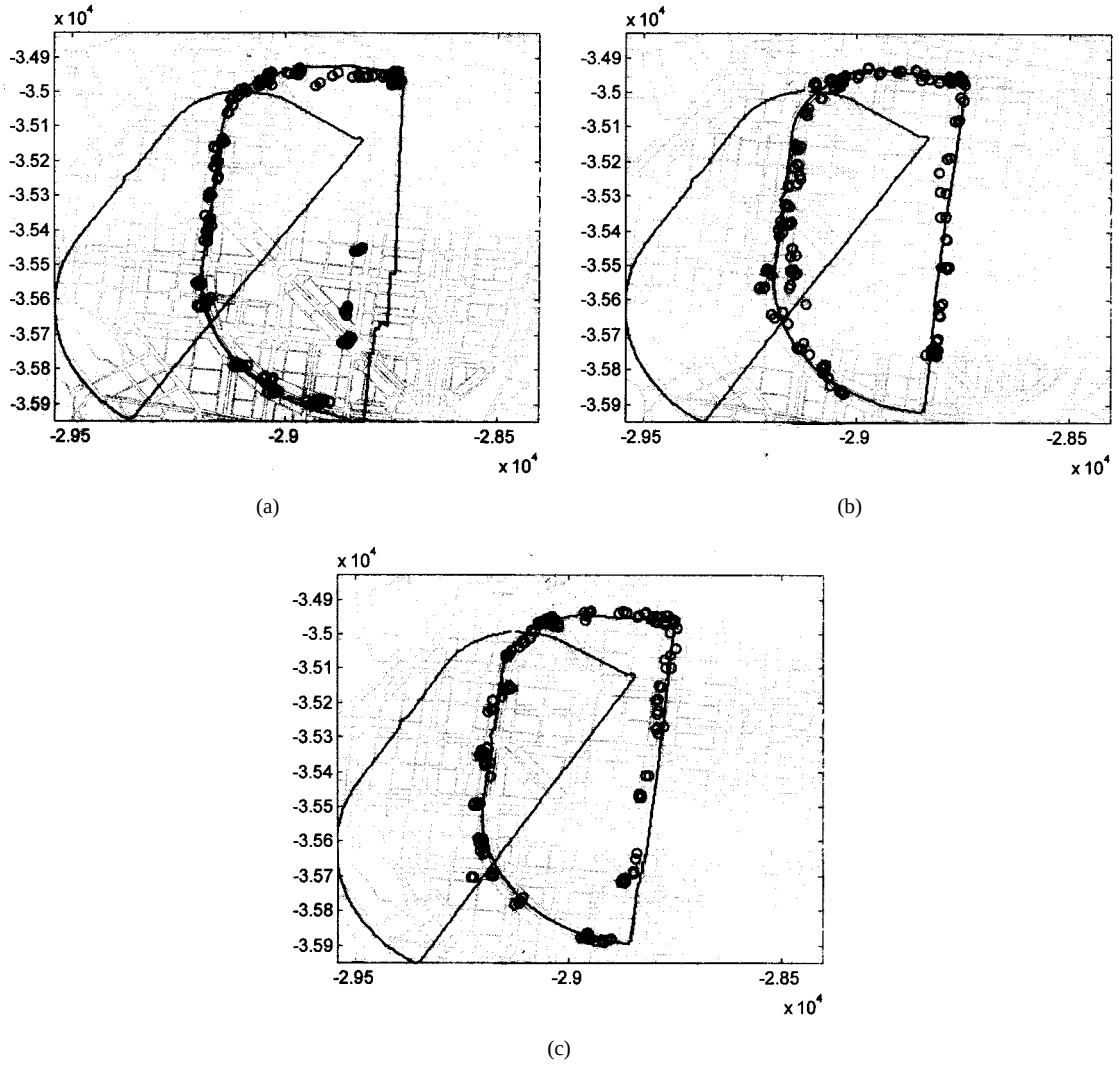

Fig. 9. (a) Trajectory estimated by the proposed FLKF method at first lap. The experimental vehicle starts from the upper right corner and travels clockwise. The FLKF converges onto the DGPS data after a short initial transient. (b) Trajectory estimated by the proposed FLKF method at second lap. The FLKF converges to the "mean" path of the DGPS data and superimposes very well onto the actual road map of the path taken by the vehicle. (c) Trajectory estimated by the proposed FLKF method at third lap. The performance of the FLKF remains accurate and consistent over time. Note the impressive extrapolation along the curvatures of the path, especially at the sharp corners and in between the sparse DGPS points.

Rate gyro: optical fiber gyro HOFG-3 Hitachi Cable, Ltd.; range: ± 100 deg/s; sensitivity: 0.05 deg/s; sampling interval: 0.5 s;

GPS receivers (2 units); HGPS-10 (HAL-lab): satellite channel: 4; position accuracy: 80–100 m (PDOP<6); receiving frequency: 1575.42 MHz (C/A code); sensitivity: 160 dBm; sampling interval: about 3 s.

Vehicle: Datsun 200ZX, Nissan Motors.

The optical-fiber gyro was mounted horizontally at the center of the vehicle, and the GPS antenna of the moving vehicle is mounted on the center of the vehicle's roof. The fixed GPS reference station was set up at a place where the radio waves could be easily received. Both the fixed and moving GPS stations received signals from the same four satellites. DGPS information, calculated from the two GPS, provides the relative distance vector for the moving vehicle with respected to the fixed station.

B. Experiments

Fig. 5 shows a two-dimensional histogram of the errors in the data from two stationary GPS's (from which DGPS information was derived) collected over a long period of time during an experiment. As can be seen in the figure, the errors in the GPS have a standard deviation of about 40 m due to the influence of the SA and do not have a zero mean. DGPS, on the other hand, has a near-zero mean error with the standard deviation only 8 meters. From the figure, the histogram of the DGPS error may be approximated by a normal distribution function.

Experiments were carried out at a Tama cemetery located in the suburbs of Tokyo. The course is shown in Fig. 6. Fig. 7 shows three sets of trajectories obtained separately by these individual instruments: 1) vehicle rate sensors; 2) GPS; and 3) DGPS. The solid line shows the trajectory from the rate sensors, the discrete data indicated by Δ are from the GPS,

and the data indicated by O are from the DGPS. The trajectory given by the rate sensors is shifted, because the initial angle θ_0 was unknown. We observe that the trajectory points given by the GPS and DGPS can sometimes be very far apart.

Fig. 8 shows more of the same results obtained from the GPS and the DGPS after the vehicle had gone around the course three times. We note that the trajectory given by the GPS is noticeably degraded by SA. The trajectory given by the DGPS is more consistent for each lap of the course, since the DGPS removes the effect of SA. However, the DGPS points are still stochastic and sparse in nature

C. Estimation of the Coordinate by the Complex Kalman Filter

Fig. 9(a)–(c) shows the trajectory estimated by the proposed FLKF method for three laps around the same test course. We observe that the filter took about half of the first lap to converge to the DGPS information. This convergence can be visualized as the rotation and translation of the rate sensor (rate gyro and speedometer) trajectory in Fig. 7 to coincide with the DGPS data in Fig 9(a). The FLKF trajectory fits accurately to the true course in the second and third laps, as shown in Fig. 9(b) and (c). We should highlight the fact that the FLKF extrapolates the path taken by the vehicle very well. This feature can be appreciated by examining the curvatures of the path, especially the sharp corners and in the spaces between DGPS points.

It is important to realize that the fuzzy logic rules and membership functions affect the Kalman filter performance in a significant way. The experimental data-driven simulation was a key factor in fine tuning the performance of the FLKF. It is also important to note that a Kalman filter without the fuzzy logic supervision will produce unacceptable estimation errors.

V. Conclusion

This paper has described how the positioning accuracy of a DGPS can be greatly improved with a vehicle speedometer and a yaw-rate gyro. The technique of sensor fusion was carried out using a complex variable version of a Kalman filter. Fuzzy logic was used to adapt the filter according to the measurement or information available. The result is a highly effective estimation technique for accurate pinpointing of vehicle position. The validity of the proposed technique was confirmed by experimental results. The fit of the FLKF trajectory over the test course was impressively accurate. The extension of the FLKF DGPS to three-dimensional positioning is currently being investigated for application to an off-road vehicle traveling over steep gradient and undulating profiles.

References

[1] D. B. Rosenblatt *et al.*, "The impact of selective availability on precise relative position with static GPS," *J. Geodesic Soc. Jpn.*, vol. 38, no. 1, pp. 29–44, 1992.
[2] R. P. K. Enge, M. Kalafusm, and M. F. Ruane, "Differential operation of the global positioning system," *IEEE Communications Mag.*, pp. 48–60, July 1988.
[3] Y. Konishi, I. Yamamoto, and H. Watanabe, "Development of compact-type Navigation System," *Jpn. Car Technol.*, vol. 46, no. 8, pp. 45–51, 1992.
[4] Y. Akazawa and T. Isobe, "Application of optical fiber gyro to vehicle," *Optronics*, pp. 79–84, Sept. 1992.
[5] A. Brown, "A multi-sensor approach to assuring GPS integrity," presented at the Annu. Assembly Meeting RTCA, 1989.
[6] K. Watanabe, K. C. Cheok, and K. Kobayashi, "Absolute speed measurement of automobile from noisy acceleration and erroneous wheel speed information," in *Proc. SAE Conf.*, Detroit, MI, Feb. 1992, pp. 75–82.
[7] K. Nishiyama, "On effectiveness of complex Kalman filter to real Kalman filter for estimation of discrete frequency spectrum," *Trans. Soc. Instrum. Contr. Eng.*, vol. 27, no. 7, pp. 776–783, 1991.
[8] T. Terano, K. Asai, and M. Sugeno, *Fuzzy Systems Theory and Its Applications*. NewYork: Academic, 1987.
[9] L. Wang, *Adaptive Fuzzy Systems and Control*. Englewood Cliffs, NJ: Prentice-Hall, 1994.
[10] D. Driankov, H. Hellendoorn, and M. Reinfrank, *An Introduction to Fuzzy Control*. Berlin, Germany: Springer-Verlag, 1993.

Kazuyuki Kobayashi received the Ph.D. degree in system engineering from Hosei University, Tokyo, Japan, in 1994.

He was a Research Associate with Oakland University, Rocheter, MI, from 1994 to 1996. Since 1996, he has been with Hosei University, where he is currently a Lecturer in the Department of System and Control Engineering. His research areas include sensing theory and signal processing and unmanned robotics, with the main emphasis on automotive applications.

Ka C. Cheok (S'80–M'82) received the B.S.E.E. degree from the University of Malaya, Kuala Lumpur, and the M.S. degree in electrical and computer engineering and the Ph.D. degree in system engineering from Oakland University, Rochester, MI, in 1977, 1979, and 1982, respectively.

He is currently a Professor in the Department of Electrical and System Engineering, Oakland University. He is active in the research areas of computer-controlled systems involving artificial intelligence and computer visualization. His contributions include the development of heuristics search, fuzzy logic, and neural network techniques for guidance of autonomous robotic vehicles, and control of active suspension, automotive traction, and tracking systems for the automotive and defense industries. He has published over 100 technical journal and conference articles. He is an Associate Editor of the *International Journal of Intelligent Automation and Soft Computing* and a Co-Organizer of the annual International Ground Robotics Competition. He served as an Operating Committee Member for the 1995 and 1977 American Control Conferences and as the General Conference Chair for the Conference on Computer Application in Industry and Engineering in 1996.

Prof. Cheok received a Michigan Teaching Excellence Award from Oakland University in 1990 and the Withdrow Teaching Excellence Award from the Oakland University School of Engineering and Computer Science in 1997.

Kajiro Watanabe received the Ph.D. degree from the Tokyo Institute of Technology, Tokyo, Japan, in 1972.

Since 1975, he has been with Hosei University, Tokyo, Japan, where he is currently a Professor and the Dean of the Department of System and Control Engineering. His research areas include sensing theory and research of controlled systems. He has published over 150 technical journal and conference articles.

Fumio Munekata received the M.S. degree in system engineering from Hosei University, Tokyo, Japan, in 1996.

He is currently with NAMCO Ltd., Kanagawa, Japan, where his work involves virtual reality.